J Appl Electrochem (2012) 42:745–751
DOI 10.1007/s10800-012-0456-7

ORIGINAL PAPER

Photo-electrochemical behavior at different wavelengths of electrochemically obtained TiO_2 nanotubes

S. Palmas · A. Da Pozzo · M. Mascia · A. Vacca · R. Matarrese · I. Nova

Received: 7 February 2012 / Accepted: 12 July 2012 / Published online: 28 July 2012

Abstract The results of an experimental study on the photo electrochemical behavior of nanotubular TiO_2 structures are presented in this work. TiO_2 samples were prepared by electrochemical anodization of Ti foils and submitted to thermal annealing. The influence of the current transient during the anodization, and of the annealing temperature on the photochemical response of the samples at different wavelengths was studied. Different behavior of the samples was observed, which may be attributed to the distributions of defects and to their different sensitivity to the temperature. The analysis of the performance of the samples in absence or in the presence of glycerol, used as hole scavenger, provided more information on the photo-catalytic properties of these structures.

Keywords TiO_2 nanotubes · Water splitting · Electrochemical oxidation · Photo-electro-catalysis

1 Introduction

The application of heterogeneous photo-catalysis based on metal oxide semiconductors for the exploitation of sunlight is one of the most important challenges that scientists are facing in the last decades. As a matter of fact, much interest has been devoted to the use of photo-catalysts for the degradation of many air pollutants, such as nitrogen oxides and volatile organic compounds, and for the reduction of the levels of greenhouse gases in the atmosphere (e.g., CO_2 and CH_4) [1]. Moreover, the photo-electrochemical water-splitting by means of solar energy has been indicated as an attractive and convenient solution to cope with environmental and energy issues related to hydrogen production [2, 3].

In this context, among the materials which have been developed for the photo-electrolysis applications, and in particular for the direct production of H_2 from solar energy and water, TiO_2 remains the most promising system, because of its superior photo-response and long-term stability as well as its low toxicity, abundance and low cost [4, 5].

The efficient use of the whole solar spectrum is one of the main topics for developing TiO_2 based-catalysts. Among the strategies for sensitizing TiO_2 to visible light, doping of titania with metal or non-metal ions was widely proposed, so that citing all the papers appeared in the literature on this topic is difficult. Numerous and wide-ranging works have been presented by several research groups such as those of Lianos, Lim, and Anpo [6–9]. However, a great debate still exists about the effectiveness of such an approach, and a lot of skepticism is highlighted about the efficiency of doped titania: in some cases the presence of the dopant is reported to create impurities that become recombination sites, thus decreasing the life-time of the photo-generated carriers [8, 9]. Actually, in these cases it could be convenient the use of well-formed active titania excited in the UV, rather than doped titania, even if this material absorbs visible light [10].

With the same goal, an appropriate control of the structure of pure titania was proposed [11]. In particular, several recent studies indicated titania nanotubes as the most attractive TiO_2 structures, thanks to their large surface

S. Palmas (✉) · A. Da Pozzo · M. Mascia · A. Vacca
Dipartimento di Ingegneria Meccanica, Chimica e dei Materiali, Università di Cagliari, Piazza D'armi, 09123 Cagliari, Italy
e-mail: simonetta.palmas@dimcm.unica.it

R. Matarrese · I. Nova
Dipartimento di Energia, Politecnico di Milano, Piazzale L. Da Vinci 32, 20133 Milan, Italy

area and efficient charge transfer. In this regard, many literature reports emphasize the unique controllable surface properties that these high-ordered architectures possess. This results in minimizing the recombination rate of the photo-generated electron–hole pairs, which represents the crucial obstacle limiting the efficiency of almost every oxide semiconductor photo-catalyst [12, 13].

Among the different routes used to make TiO_2 nanotubes, electrochemical oxidation of titanium foils in solutions containing fluorides as corrosion agents has been demonstrated to be a very simple and effective method to obtain self-organized oxide nanotube arrays [14–16].

Most of the recent studies focused on the control of the nanotube morphology, namely nanotube length, diameter, and wall thickness: electrolyte composition and pH, as well as the anodization potential were found as key factors in controlling the geometrical features of the nanotube arrays [17, 18]. Furthermore, the thermal annealing process, used to transform the amorphous into crystalline structures, was proved to influence the final structure and composition of TiO_2 nanotubes [19].

In this context, an experimental study has been recently undertaken in our laboratories in order to investigate the working mechanism of non-doped TiO_2 nanotubes prepared by anodic oxidation of Ti foils either in aqueous [20–22] or in organic electrolytes [23], always containing fluorides. Emphasis was given to the parameters which were found to influence the formation and the photo-response of the nanotubular arrays. In particular, the effects of both anodization time and annealing process (e.g., temperature and atmosphere) on the final structure of TiO_2 nanotubes were examined, focusing on both the related crystalline phase transformations and the presence of structure defectiveness at the surface or in the bulk.

In addition, the nature and distribution of superficial states originated during the anodization process were found to depend on the initial surface roughness as well as on the presence of hydroxide nano-islands that could be crucial for the surface pit initiation and the subsequent growth of nanotubes [21, 24].

The present work aims to contributing to the research in this field, widening the knowledge about the relationship between the different structures of the starting material and the final behavior of the sample irradiated by light at different wavelengths. Actually, it must be considered that most of the investigations carried out so far in our laboratory, as well as most of the works present in the literature concerning nanostructured titania, were focused on the photo-activity of the samples in the UV range, where TiO_2 has its best performance. In view of a possible optimization of the process and its addressing to practical applications capable to exploit a wider range of the solar spectrum, it is useful to widen the field of investigation to different wavelengths of incident radiation. The present study investigates in particular a wavelength range from 340 to 400 nm, with experiments specifically designed to evaluate whether and to what extent the differences in the structure of the starting samples, in terms of different distribution of bulk and surface defects, could justify the differences in behavior observed for samples irradiated at different wavelengths of the incident light.

2 Experimental procedure

Samples were obtained by electrochemical anodization of Ti foils (0.25 mm thick, 99.7 % metal basis, Aldrich) according to a previously reported procedure [21]. The oxidation was preceded by cleaning and degreasing of the foils which were sonicated in acetone, isopropanol and methanol; they were then rinsed with deionized water and dried in a nitrogen stream. The pre-treated samples were then submitted to electrochemical anodization in fluoride containing aqueous solution (0.4 M NH_4NO_3 + 0.25 M NaF). A three electrode cell was used in which the Ti sample worked as anode, a platinum grid worked as counter electrode and a saturated calomel electrode (SCE) as reference: all the values of potential in the text are referred to SCE. All the samples were oxidized at 20 V: a potential ramp was applied from open circuit voltage (OCV) to 20 V with a scan rate of 100 mV s^{-1}; then, the applied potential was maintained at this fixed value for 3 h. After oxidation, the electrodes were rinsed in deionized water and dried in a nitrogen stream. Water cool recirculation was maintained during the run in order to keep the temperature at 20 °C. Two different temperatures were used in the annealing treatments, performed in air atmosphere for 1 h: 400 and 600 °C.

The morphology and the phase composition of the samples were characterized by SEM, TEM and XRD analyses. Details can be found elsewhere [21]. Ordered nanotubular structures were detected in all the experimental conditions with average inner and outer nanotubes diameters in the range of 75 ± 5 and 95 ± 5 nm, and nanotube length in the order of 1 μm. No appreciable differences were obtained regardless of the relative concentration of the superficial and bulk defects and the annealing temperature.

XRD patterns indicated the presence of a unique anatase phase in all the samples treated at 400 °C while low percentages (from 2 to 5 % in weight) of rutile were found in those treated at 600 °C.

Different values of OCV were measured for the different samples, in the range from −0.6 to −0.65 V versus SCE for the samples annealed at 400 °C and in the range from −0.65 to −0.7 V versus SCE for the samples annealed at 600 °C.

Photocurrent measurements were performed with the same electrochemical cell used for Ti anodization: in this case TiO_2 samples (nominal area 1 cm^2) worked as anode.

The photocurrent experiments consisted in potential ramps from OCV to about 1.2 V, at a constant scan rate of 5 mV s^{-1}, in the dark and under illumination. The value of photocurrent was obtained as the difference between light and dark currents.

The light source was a 300 W Xe lamp (Lot Oriel): the behavior of the samples was studied using four filters with center wavelength at 340, 365, 380 and 400 nm and bandwidth of 10.83, 9.45, 10.84 and 18 nm respectively. Depending on the filter used, different powers (P) of the light, in the range between 1.5 and 11 mW cm^{-2}, arrived at the electrode surface. Thus, a direct comparison of the performances at the different wavelengths was made in terms of photocurrent normalized with respect to the incident power light ($i_P = i/P$).

All the experiments were carried out in a KOH (0.1 M) electrolyte, or with the addition of glycerol 0.1 M where indicated.

3 Results and discussion

The preparation of TiO_2-based nanotubular structures electrochemically grown on Ti foil has been studied for some years in our laboratories. Among the interesting results obtained during the synthesis and the characterization of a large number of samples, certainly worthy of note is the poor reproducibility of the synthesis. Maybe even due to superficial inhomogeneity of the starting titanium foils, samples obtained under the same oxidative conditions can have different behaviors in the anodization curves [21]. Actually, a peak at 3 V was always present in the I versus E curves during the first potential ramp, but, depending on the case, its value was higher or lower than the steady state current recorded during the subsequent potentiostatic step at 20 V. So, the behavior of the samples has been correlated to the shape of the related anodization curve, rather than to the operative conditions adopted in the synthesis. In particular, a parameter f was defined as the ratio between the current measured at the steady state at 20 V (i_{20}), and that registered at the peak at 3 V (i_3); these current values were found to be an indication of the concentration of superficial and bulk defects, respectively. So a value of f greater than unity indicated the prevalence of superficial states, whereas f values lower than unity could be correlated to the samples at which bulk defects were prevailing [21].

The same parameter f resulted effective in order to differentiate the trends of data related to the Mott Schottky (MS) analysis used to characterize the electronic structure of the samples [21]. Quite linear MS plots were obtained for samples with $f > 1$, which also showed the highest values of donor concentration (N_D in the order of 10^{20} cm^{-3}), while for samples derived from anodization curves with $f < 1$, changes in the slopes of the MS plots were measured, which were generally attributed to a variation in the energy levels of the sites involved during the potential scan. Lower N_D values were also measured for these samples, in the order of 10^{18} cm^{-3}. All the tests have been carried out at the wavelength of 365 nm.

This work aims to complete the characterization of those samples by testing their behavior in a wider range of wavelengths in order to investigate how the parameter f can be related to the differences in the performances observed at the different wavelengths.

The prepared samples were divided into two classes, A and B, to indicate those with f greater and lower than 1, respectively. The f values, as well as the annealing temperature of all the investigated samples, are reported in Table 1.

Considering the performances of the samples, the trends of photocurrents measured at the different λ, for samples of A and B classes annealed at 400 and 600 °C are presented in the following.

As pointed out in the experimental section, different OCV values were measured for the different samples, so that, for a better comparison, data are reported as a function of E_{app}, which represents the difference between the bias potential E and the OCV under the irradiated power light. This difference is also of particular significance because it represents a crucial parameter in the energetic yield of an electrically driven photo-process, in which the net power output obtained is taken into account [25]:

$$\varepsilon = i_p(E^0_{rev} - |E_{app}|) \quad (1)$$

where $E^0_{rev} = 1.23$ V is the standard reversible potential for water splitting, and i_P is the normalized photocurrent with respect to the incident power light.

The comparison between samples annealed at 400 °C (Figs. 1, 2) shows that, for the same potential, photocurrents decrease with the increasing wavelength, according to the change in the absorption coefficient of the TiO_2.

However, as it can be seen from Figs. 3 and 4, the trend is not so regular if we consider the currents recorded for the

Table 1 Samples used in the experiments

Class of samples	f	Sample	Annealing temperature, T_a (°C)
A	2.1	S1	400
	1.5	S2	600
B	0.4	S3	400
	0.3	S4	600

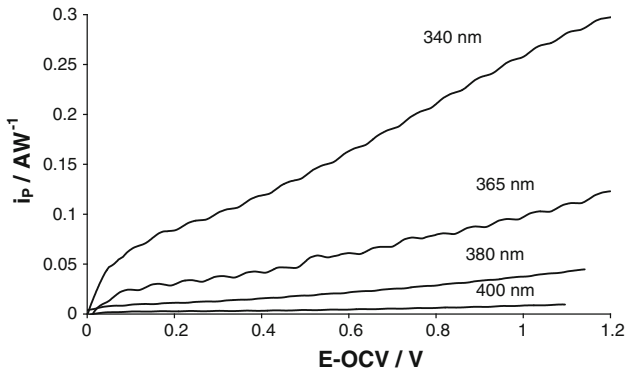

Fig. 1 Trend of photocurrents (normalized with respect to incident light power) versus overpotential, for the sample S1, annealed at 400 °C

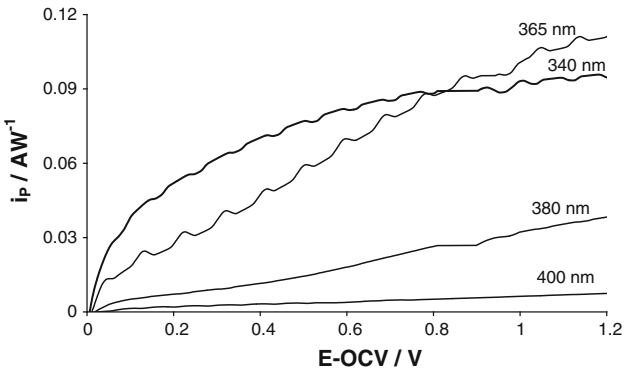

Fig. 3 Trend of photocurrents (normalized with respect to incident light power) versus overpotential, for the sample S2, annealed at 600 °C

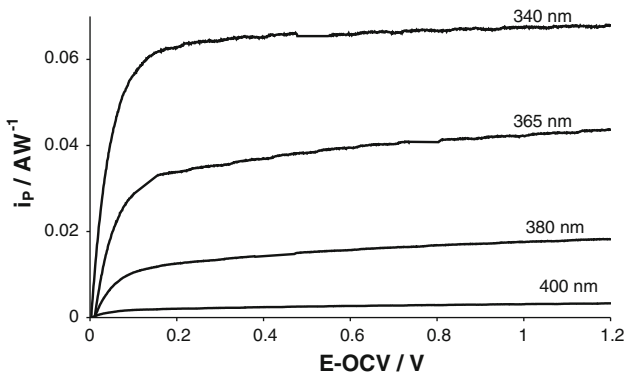

Fig. 2 Trend of photocurrents (normalized with respect to incident light power) versus overpotential, for the sample S3, annealed at 400 °C

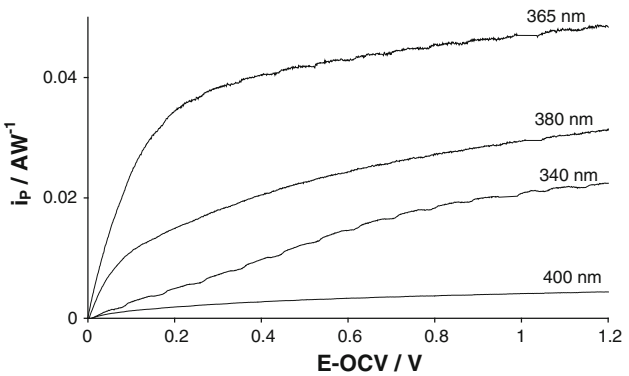

Fig. 4 Trend of photocurrents (normalized with respect to incident light power) versus overpotential, for the sample S4, annealed at 600 °C

samples treated at 600 °C: this is particularly evident for the sample S4 at which the current recorded at 340 nm is lower than that recorded both at 365 nm and at 380 nm.

The role of the annealing has to be particularly approached. Important effects on the morphology and/or on the crystalline phases could be expected with temperature variation. However, as pointed out in the experimental part, in this case analyses did not show significant variations in the morphology of the samples annealed at different temperatures. Annealing temperatures up to 600 °C were also reported in the literature as not substantially influencing the morphology of the nanotubes [19]. Also, slight effects were reported to start at 600 °C [26]. In our case, the short time of the annealing treatment could have prevented any significant variation from occurring.

Moreover, at the highest temperature a more complete transformation from amorphous to crystalline structure should be expected, and above 600 °C the transformation from anatase to rutile should also begin, which has been demonstrated to have beneficial effects on the photocurrents [10, 27]. However, the partial transformation to rutile revealed in our samples does not seem to be sufficient to justify the trends observed at the different wavelengths.

Our results highlight that the effect of the temperature cannot be considered as such: a complex effect of temperature, distribution of defects, and wavelength of the incident radiation has to be simultaneously considered.

To simplify the comparison of the obtained data, the ratio **j** between the photocurrent responses at samples of the same class annealed at 400 °C (I_{400}) and those annealed at 600 °C (I_{600}) has been compared at two different overpotential values and at the different wavelengths. The corresponding data are listed in Table 2.

If the data obtained at $\lambda \geq 365$ nm are compared, results show that the increase in temperature has a beneficial effect in the performance (values of $j < 1$) only for samples of class B. For A samples, annealing at the highest temperature seems to have no or even slightly negative effect ($j \geq 1$).

In any case, for both classes of samples, the most significant and negative effect is that at 340 nm wavelength, at which the photocurrent recorded for the samples

Table 2 j values obtained at the different wavelengths and at two different overpotentials for the two classes of samples

$j = I_{400}/I_{600}$	Wavelength (nm)			
	340	365	380	400
A samples $f > 1$				
$E_{app} = 0.5$ V	1.8	1	1.1	1
$E_{app} = 1$ V	3.2	1	1.1	1
B samples $f < 1$				
$E_{app} = 0.5$ V	5.4	0.9	0.7	0.8
$E_{app} = 1$ V	3.2	0.9	0.8	0.8

annealed at the highest temperature shows values up to five times lower than those obtained for the samples annealed at 400 °C.

In order to derive further information on the process, and in particular to verify how recombination is affecting the process for samples annealed at the highest temperature, additional data were derived from electrolyses carried out in the presence of a hole-scavenger such as glycerol for both classes of samples. Figure 5 shows the normalized photocurrent values at the fixed overpotential of 0.5 V, obtained for samples S2 (class A) and S4 (class B), both annealed at 600 °C.

The positive effect of the hole scavenger on the recorded photocurrents indicates that recombination of the photo-generated charges takes place, to a more or less extent, at all the wavelengths. It is worth to observe that the effect of glycerol is more evident at lower wavelengths, supporting the greater extent of superficial recombination.

Finally, it is noteworthy that for sample S2, characterized by the presence of a large amount of superficial defects, the presence of glycerol was able to restore the downward trend of photocurrent values with increasing λ, which was observed for the samples annealed at 400 °C.

A different response was obtained for the S4 sample: despite the positive effect of glycerol, the photocurrent at 340 nm remained lower than that recorded at 365 nm. This result can be taken as an indication of a different ability of the surfaces of the two samples to adsorb glycerol. A preferential sorption of glycerol at superficial rather than at bulk states, may explain the higher response in photocurrent for sample S2.

In order to justify the photo-activity of the titanium dioxide, such defects, as oxygen vacancies, Ti vacancies and interstitial Ti, have to be taken into account [28–30]. In particular, oxygen vacancies or interstitial Ti, which are donors by their nature, correspond to energetic levels near to the conduction band; Ti vacancies, which are acceptors, correspond to energetic levels near to the valence band. This last kind of defects is easily formed at the oxide surface, and then they tend to move to the bulk via a very slow diffusing process [30, 31].

The presence of such a defective structure may strongly influence the response of the system to an applied potential. In the simplest case of absence of superficial states, when a potential more positive than the flat band potential is applied in the dark, the resulting effect is a displacement of the Fermi level and a band bending in the space charge region. In the presence of defects and superficial states, when the potential applied is at least corresponding to a superficial state, its depletion starts and the Fermi level is pinned up to the complete empting of the states. At the end, if the electric field is sufficiently high, the released electrons migrate to the bulk and the holes to the surface, so that the surface becomes less negative and the depletion decreases. In the presence of light the behavior is different. If the radiation has enough energy, electrons are injected in the conduction band, but also electron jumps from valence band to empty acceptors levels or from superficial states to

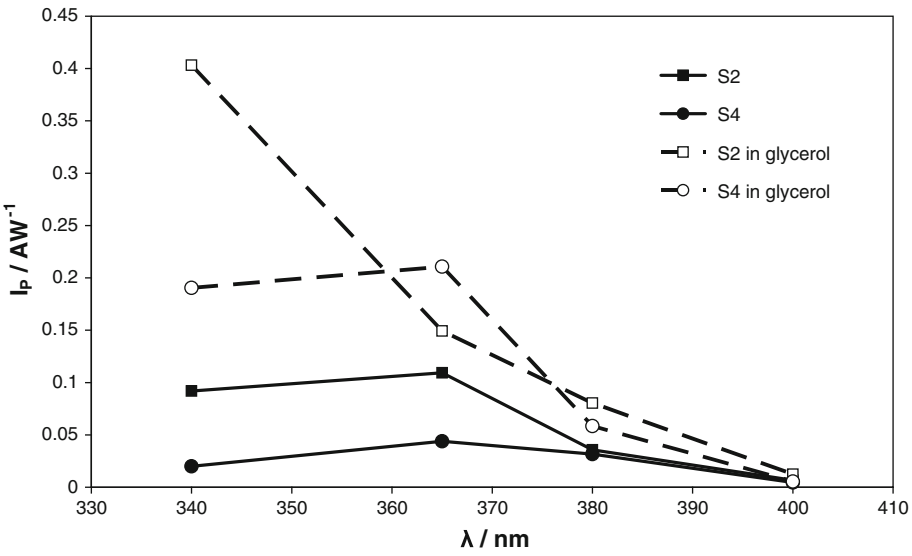

Fig. 5 Effect of glycerol on the trend of normalized photocurrents versus wavelength, for samples S2 and S4. $E_{app} = 0.5$ V

the conduction band are possible. In particular, the main effect of donor levels may be an increase in the electrical conductivity due to the electrons injected in the conduction band, but also a decrease in the band bending, so that the electrons arriving in the conduction band have a higher probability to be recombined with holes. The effect of acceptor levels is to trap the electrons at the surface, but also to increase the band bending and then to increase the separation of the photo-generated charges.

Depending on the relative concentration of the two kinds of defects and on the energy associated to the wavelength, a positive or negative effect on the photo-activity can be dominant.

As shown in Figs. 1–4, a comparison between the measured values of photocurrent indicates that the highest currents are obtained with the A samples at which a high concentration of superficial states should be originated during Ti oxidation ($f > 1$). Moreover, apart from the data measured at 340 nm, the current values obtained with the A samples did not appreciably change for samples annealed at 400 or 600 °C (as shown in Table 2, values of j always around unity were measured with the samples A). The donor character of the superficial states may justify the observed trend. Actually, for A samples, thermal treatment at 600 °C removes a certain amount of defects; but since they were initially at very high concentration, their variation may be not so much outstanding. The resulting sample is still highly conductive, and at all wavelengths $\lambda \geq 365$ nm photocurrents regularly increase with the increase in the applied potential, without appreciable saturation current. Results obtained in the presence of glycerol indicate that a certain percentage of recombination is present also at these wavelengths: the band bending created by the acceptor sites present in the structure may not be sufficient to separate all the generated charges.

A different behavior is obtained at 340 nm, at which the sample treated at higher temperature seems to lose most of its photo-activity. This result could be explained by considering that the thermal treatment can have a second effect, accelerating the slow diffusion process of the Ti vacancies toward the bulk system. This is the most important effect at 340 nm: actually, this wavelength may not be penetrating enough to involve Ti vacancies, so that they remain empty and the surface less negatively charged. Thus, a lower band bending is originated, which is no more able to separate the photogenerated charges. Data in glycerol confirm the pronounced effect of recombination at this wavelength.

The behavior of the B samples may be understood by considering that the prevailing sites in these samples should be the bulk ones ($f < 1$); superficial sites are present in less extent so that the photocurrent is generally lower than in the previous case.

At the highest wavelengths a quite positive effect on the photocurrent for samples treated at 600 °C can be highlighted (Table 2): these data indicate that the prevailing character of bulk defects is acceptor, and in this case, their positive contribution can be highlighted, because the contribution of the superficial sites is less dominant than in the previous case.

However, also in this case, annealing at 600 °C has two effects: it reduces the superficial defects, and once more it accelerates the diffusion of Ti vacancies to the interior of the film. This last fact, in turn, may be also responsible for the strong decrease of the current at 340 nm.

4 Conclusions

The analysis of data herein presented revealed a complex and synergistic interaction of several factors on the photoelectrocatalytic properties of TiO_2 nanotubes arrays.

Defect concentration and distribution are highly influent on the photocurrent response. Energetic levels near to the conduction band edge or deeper inside the band gap were associated with superficial and bulk defects, respectively. Their concentration and distribution resulted strongly influenced by the annealing temperature. The main effect of an increase in the annealing temperature is a decrease in the concentration of superficial sites, which in turn decreases the concentration ratio of the superficial to bulk sites. This fact has a direct consequence on the response of the system to the applied potential, and to the wavelength of the incident light. Superficial sites seem to be mostly responsible for the conductivity of the samples, while deeper defects could be strongly effective in determining the behavior at different wavelength. In particular, the diffusion from surface to bulk of Ti vacancies accelerated by the higher temperature seems responsible for the different behavior observed for all the samples at the lowest wavelength (340 nm).

References

1. De Richter R, Caillol S (2011) Fighting global warming: the potential of photocatalysis against CO_2, CH_4, N_2O, CFCs, tropospheric O_3, BC and other major contributors to climate change. J Photochem Photobiol C 12:1
2. Kudo A, Miseki Y (2009) Heterogeneous photocatalyst materials for water splitting. Chem Soc Rev 38:253
3. Chen X, Shen S, Guo L, Mao SS (2010) Semiconductor-based photocatalytic hydrogen generation. Chem Rev 110:6503
4. Linsebigler AL, Lu G, Yates JT Jr (1995) Photocatalysis on TiO_2 surfaces: principles, mechanisms, and selected results. Chem Rev 95:735
5. Fujishima A, Zhang X, Tryk DA (2008) TiO_2 photocatalysis and related surface phenomena. Surf Sci Rep 63:515
6. Lianos P (2011) Production of electricity and hydrogen by photocatalytic degradation of organic wastes in a photoelect-

rochemical cell: the concept of the photofuelcell: a review of a re-emerging research field. J Hazard Mater 185:575
7. Akpan UG, Hameed BH (2010) The advancements in sol–gel method of doped-TiO_2 photocatalysts. Appl Catal A Gen 375:1
8. Lim M, Zhou Y, Wang L, Rudolph V, Lu(Max) GQ (2009) Development and potential of new generation photocatalytic systems for air pollution abatement: an overview. Asia Pac J Chem Eng 4:387
9. Ji P, Takeuchi M, Cuong T-M, Zhang J, Matsuoka M, Anpo M (2010) Recent advances in visible light-responsive titanium oxide-based photocatalysts. Res Chem Intermed 36:327
10. Bouras P, Stathatos E, Lianos P (2007) Pure versus metal-ion-doped nanocrystalline titania for photocatalysis. Appl Catal B 73:51
11. Rani S, Roy SC, Paulose M, Varghese OK, Mor GK, Kim S, Yoriya S, LaTempa TJ, Grimes CA (2010) Synthesis and applications of electrochemically self-assembled titania nanotube arrays. Phys Chem Chem Phys 12:2780
12. Nowotny J, Bak T, Nowotny MK, Sheppard LR (2007) Titanium dioxide for solar-hydrogen I functional properties. Int J Hydrogen Energy 32:2609
13. Sang LX, Zhang ZY, Ma CF (2011) Photoelectrical and charge transfer properties of hydrogen-evolving TiO_2 nanotube arrays electrodes annealed in different gases. Int J Hydrogen Energy 36:4732
14. Grimes CA (2007) Synthesis and application of highly ordered arrays of TiO_2 nanotubes. J Mater Chem 17:1451
15. Macak JM, Tsuchiya H, Ghicov A, Yasuda K, Hahn R, Bauer S, Schmuki P (2007) TiO_2 nanotubes: self-organized electrochemical formation, properties and applications. Curr Opin Solid State Mater Sci 11:3
16. Roy P, Berger S, Schmuki P (2011) TiO_2 nanotubes: synthesis and applications. Angew Chem Int Ed 50:2904
17. Mor GK, Varghese OK, Paulose M, Shankar K, Grimes CA (2006) A review on highly ordered, vertically oriented TiO_2 nanotube arrays: fabrication, material properties, and solar energy applications. Sol Energy Mater Sol Cells 90:2011
18. Ghicov A, Schmuki P (2009) Self-ordering electrochemistry: a review on growth and functionality of TiO_2 nanotubes and other self-aligned MO(x) structures. Chem Commun 20:2791
19. Yu J, Wang B (2010) Effect of calcination temperature on morphology and photo-electrochemical properties of anodized titanium dioxide nanotube arrays. Appl Catal B 94:295
20. Palmas S, Polcaro A, Rodriguez Ruiz J, Da Pozzo A, Mascia M, Vacca A (2010) TiO_2 photoanodes for electrically enhanced water splitting. Int J Hydrogen Energy 35:6561
21. Palmas S, Da Pozzo A, Mascia M, Vacca A, Ardu A, Matarrese R, Nova I (2011) Effect of the preparation conditions on the performance of TiO_2 nanotube arrays obtained by electrochemical oxidation. Int J Hydrogen Energy 36:8894
22. Palmas S, Da Pozzo A, Mascia M, Vacca A, Ricci PC, Matarrese R (2012) On the redox behaviour of glycerol at TiO_2 electrodes. J Solid State Electrochem 16(7):2493
23. Palmas S, Da Pozzo A, Delogu F, Mascia M, Vacca A, Guisbierg G (2012) Characterization of TiO_2 nanotubes obtained by electrochemical anodization in organic electrolytes. J Power Sources 204:265
24. Al-Abdullah ZTY, Shin YY, Kler R, Perry CC, Zhou WZ, Chen QA (2010) The influence of hydroxide on the initial stages of anodic growth of TiO_2 nanotubular arrays. Nanotechnology 21:50
25. Varghese OK, Grimes CA (2008) Appropriate strategies for determining the photoconversion efficiency of water photoelectrolysis cells: a review with examples using titania nanotube array photoanodes. Solar Energy Mater Sol Cells 92:374
26. Liu R, Yang WD, Qiang LS, Wu JF (2011) Fabrication of TiO_2 nanotube arrays by electrochemical anodization in an NH_4F/H_3PO_4 electrolyte. Thin Solid Films 519:6459
27. Yan M, Chen F, Zhang J, Anpo M (2005) Preparation of controllable crystalline titania and study on the photocatalytic properties. J Phys Chem B 109:8673
28. Nowotny J, Bak T, Nowotny MK, Sheppard LR (2007) Titanium dioxide for solar-hydrogen. II. Defect chemistry. Int J Hydrogen Energy 32:2630
29. Nowotny J, Bak T, Nowotny MK, Sheppard LR (2007) Titanium dioxide for solar-hydrogen. III. Kinetic effects. Int J Hydrogen Energy 32:2644
30. Nowotny J, Bak T, Nowotny MK, Sheppard LR (2007) Titanium dioxide for solar-hydrogen. IV. Collective and local factors in photolysis of water. Int J Hydrogen Energy 32:2651
31. Nowotny MK, Bak T, Nowotny J, Sorrell CC (2005) Titanium vacancies in nonstoichiometric TiO_2 single crystal. Phys Status Solidif B 242:R88